Bulgarian Chemical Communications, Volume 49, Special Issue A (pp. 7–20) 2017

Crystal chemistry and structural characterization of natural Cr-spinels

I. S. Sergeeva[1]*, T. N. Kerestedjian[1], R. P. Nikolova[2],
Z. P. Cherkezova-Zheleva[3], F. Gervilla[4]

[1] *Geological Institute "StrashimirDimitrov", Bulgarian Academy of Sciences, Acad. G Bonchev str., bl. 24, 1113 Sofia, Bulgaria*
[2] *Institute of Mineralogy and Crystallography "Acad. Ivan Kostov", Bulgarian Academy of Sciences, Acad. G. Bonchev str., bl.107, 1113 Sofia, Bulgaria*
[3] *Institute of Catalysis, Bulgarian Academy of Sciences, Acad. G Bonchev str., bl. 11, 1113 Sofia, Bulgaria*
[4] *Departamento de Mineralogıa y Petrologıa, Universidad de Granada-CSIC, Avda.Fuentenueva s/n, 18002 Granada, Spain*

Received October, 2016; Revised December, 2016

Two natural chromian spinel samples were examined by means of electron microprobe chemical analysis (EPMA), powder X-ray diffraction, single-crystal X-ray diffraction and Mössbauer spectroscopy, in order to reveal some aspects of the relationships between composition and structural parameters. The samples originate from the East Rhodopean serpentinite massive of Golyamo Kamenyane in Bulgaria, which is part of a dismembered ophiolite complex. The two samples differ significantly in textural, chemical and structural respect. One of the samples is chromium rich and can be regarded as Cr-spinel, whereas the other one is very rich in Fe^{2+} and Fe^{3+} (as shown by EMPA and Mössbauer spectroscopy), approximating magnesioferrite end member of the spinel group. These contrasting compositional differences result in very pronounced differences in structural parameters – unit cell parameter and *u* oxygen positional parameter, which reflect different conditions of formation and/or alteration. The *u* parameter is indicative for the thermal history of the hosting ultramafic rock. It depends on cation distribution, but not very strongly, which allows rather accurate determination of *u* within reasonable limits of cation distribution uncertainty. Nevertheless, our results show, that diffraction studies alone are insufficient for geothermometric purposes and have to be combined with EPMA and Mössbauer data. Calculated system closure temperatures for both samples indicate 796–1073 °C, which are acceptable for the Cr-spinel reequilibration conditions on cooling. For outer rims of the crystals, however, as well as for the iron rich sample, formed during later metamorphic events, lower temperatures should be expected.

Keywords: Cr-spinels, X-ray diffraction, structural parameters.

INTRODUCTION

The natural Cr-spinels belong to the group of 2-3 oxide spinels with general formula AB_2O_4, where:

- tetrahedrally coordinated cations A = Mg, Fe^{2+}, Zn, Mn^{2+}, etc.
- octahedrally coordinated cations B = Cr, Al, Fe^{3+},Ti^{4+}, V^{3+}, Co, etc.

Two fully ordered cation distributions are known in spinels: normal $A[B_2]O_4$ for ideal chromite and inverse $B[AB]O_4$ for ideal magnetite. A and B represent divalent and trivalent cations respectively, occupying the tetrahedrally (round or no brackets) and octahedrally (square brackets) coordinated sites, whereas O is anion (oxygen) site in the structure. Intermediate cation distributions, are expressed with the structural formula:

- $(A_{1-x}B_x)[A_xB_{2-x}]O_4$, where x denotes inversion parameter

In the normal spinel x is equal zero and in the inverse one – unity [1].

The inversion parameter, x, is defined as the fraction of B-type cations in the tetrahedral site (A).

Both Cr-spinel and magnetite are a common constituent of serpentinized and metamorphosed ultramafic rocks, especially in ophiolite complexes [2–4]. Distinguishing of these mineral species, based on chemical criteria alone is insufficient, since both chromium containing magnetite and high iron Cr-spinel are common in metamor-

* To whom all correspondence should be sent:
E-mail: sergeevai@geology.bas.bg

phosed/serpentinized peridotites. The only way to identify the species is by determination of the inversion parameter.

The differentiation of both species is crucial for geological interpretation, since Cr-spinel is a typical magmatic product, while magnetite is commonly formed during later, serpentinization alteration or even late hydrothermal events. The availability of overprinting regional metamorphic events, altering the initial, pristine Cr-spinel and pretty common in such environment, additionally complicates the interpretation of observed mineral relations.

Another important parameter is the oxygen positional parameter *u* which can be used for determination of system closure temperature, important for the genetic interpretation of the mineral forming processes [4–7]. The determination of this parameter value requires prompt determination of cation distribution in first order.

In this paper, the crystal chemistry of two natural Cr-spinels from Golyamo Kamenyane serpentinite was studied by multiple methods in order to explore the composition – structure relations. Both unit cell parameter *a* and oxygen positional parameter *u* depend on cation distribution in tetrahedral and octahedral sites of the spinel structure. However, complex chemistry of natural spinels hampers the correct determination of cation distribution with a single research method. This is why we employ a number of supporting methods. In addition, the reliability of structural interpretations was checked by applying two independent X-ray diffraction studies – powder and single crystal.

GEOLOGICAL SETTING

The Golyamo Kamenyane serpentinite is part of a dismembered metaophiolite, located in the Avren synform, in the Upper High-Grade Unit of the metamorphic basement of Eastern Rhodopean crystalline massif, in South Bulgaria [8–10] (Fig. 1).

Metamorphism of these rocks had reached eclogite-facies conditions (up to 13–16 kbar and 600 °C) followed by variable retrogressive P–T trajectories [11–13] down to greenschist-facies conditions. This unit also includes scattered bodies of ultramafic rocks (partly serpentinized peridotites, locally preserving garnet-bearing assemblages [14].

Although the metamorphic conditions of the Golyamo Kamenyane serpentinite are not calculated yet, according to Kozhoukharova [15], amphibolitized eclogites from the Avren synform had reached 12–17 kbar and 750–811 °C.

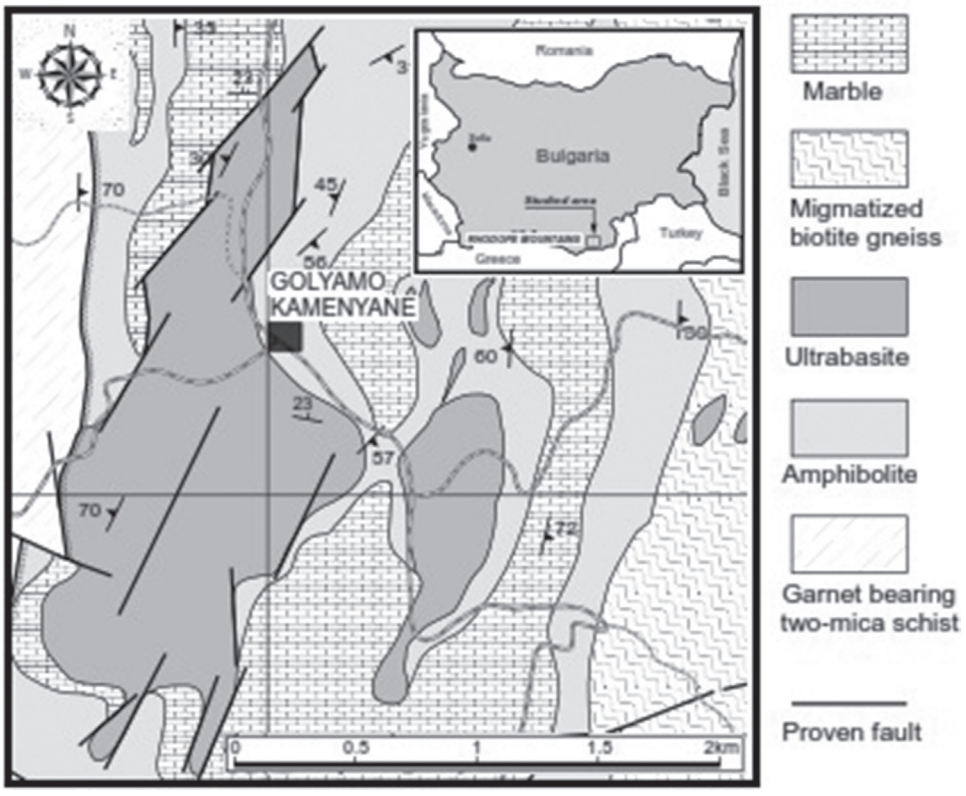

Fig. 1. Geological map of the Golyamo Kamenyane serpentinite and nearby areas (modified from Sarov et al. 2007).

MATERIALS AND METHODS

Sampe description and sample preparation

The Cr-spinels studied were extracted from chromite ore bodies (chromitites) which show massive (> 85 vol. % Cr-spinel) and semi-massive (60-85 vol. % Cr-spinel) textures. The massive chromitite is coarse grained, relatively homogeneous with minor inclusions of antigorite, whereas, the semi-massive one is associated with considerable amount of chlorite (Cr-clinochlore), filling the interstitial grain spaces and forming coatings around Cr-spinel grains.

Cr-spinel and silicate fractions were separated from all samples for XRD and Mössbauer spectroscopy analysis. The procedure involves grinding, sieving and combined magnetic and gravity separation in a vibrating micro-panner and bromoform column sedimentation.

Electron probe micro analysis

The Cr-spinel samples were studied by environmental scanning electron microscope (ESEM) in backscattered electron (BSE) mode prior to microprobe analysis (EPMA).

Spots for analysis were selected on BSE images, along core to rim cross-sections, in order to reveal the chemical composition of all alteration zones.

Chemical compositions were obtained using a CAMEBAX SX100 at the Centro de Instrumentación Científica of the University of Granada (Spain) under an excitation voltage of 20 kV and a beam current of 20 nA, with a beam of 2–3 μm in diameter. Monitored spectral lines were MgKα, FeKα, AlKα, CrKα, SiKα, TiKα, MnKα, NiKα and VKα. Standards used were MgO, Fe_2O_3, Al_2O_3, Cr_2O_3, SiO_2, TiO_2, $MnTiO_3$, NiO and $Pb_5(VO_4)_3Cl$. Structural formulae of Cr-spinel were calculated assuming stoichiometry, with correction from C-J De Hoog[17].

Mössbauer spectroscopy

Mössbauer spectra were collected at 297 K in transmission mode, using a conventional constant acceleration spectrometer (Wissenschaftliche Elektronik GMBH, Germany), and a 50 mCi ^{57}Co/Rh source. The velocity scale was calibrated according to the centroid of reference spectrum of α-Fe foil at room temperature. Mössbauer absorbers were prepared from powdered Cr-spinel samples pressed into sample holder. The experimental spectra were analyzed using least-squares program CONFIT [18], which allows evaluation of registered Mössbauer spectra with Lorenzian peak shape.

The refined parameters of hyperfine interactions were isomer shift (IS), quadrupole splitting (QS) and effective internal magnetic field (H_{eff}). Line broadening (FWHM) and relative weight of partial components (G) were also obtained. The highest convergence of experimental and theoretical spectra was accepted for the best fit.

Powder X-ray diffraction

The separated monomineralic fractions from Cr-spinel samples were grinded in agate mortar with alcohol to obtain fine suspension. The suspension was then finely deposited on thin Mylar foil, stretched onto sample holder.

X-ray powder diffraction analyses were carried out using HUBER Guinier Image Plate Camera G670 in asymmetric transmission mode, with Cu $K\alpha_1$ radiation, in the range 4–100 degrees and step size of 0.005 2θ at the Geological Institute of the Bulgarian Academy of Sciences. Diffraction data were treated with MATCH! software package for phase analysis, by CRYSTAL IMPACT, Bonn, Germany[19].

The Rietveld structure refinement was performed with FULLPROF Suite Program, by Juan Rodrigues Carvajal [20]. Structural parameters were refined within the space $Fd\bar{3}m$ group with origin at $\bar{3}m$ position and tetrahedral ions placed in 8(*a*) position; octahedral ions in 16(*d*) and oxygen ions in 32(*e*) position. The refined parameters were zero shift, scale factor, unit cell parameters, oxygen positional parameter, occupation factors for both – tetrahedral and octahedral sites and isotropic thermal displacement parameters (B) for both cationic positions and oxygen (anionic) positions. Pseudo Voigt and TCH profile functions were used for approximation of the peak shape. The background curve was modeled using linear interpolation between manually selected background points from the raw diffraction pattern. This procedure shows very good background approximation. Data from EPMA and Mössbauer spectroscopy (Fe^{2+}/Fe^{3+} distribution) were used as starting model for the Rietveld refinement. Preferred cation positions were chosen on the basis of literature data [21, 22]. Initial unit cell parameters were taken from the closest database match, proposed by MATCH! phase identification software. In order to avoid unnecessary complexity of the refinement procedure, the minor element (Ti, V, Ni, Mn) contents were fixed at values obtained from EPMA. The isotropic thermal displacement parameters in one of the samples (GK1A-7) were refined at the end of the procedure, with all previously refined parameters fixed, because very strong correlations were observed. These correlations were attributed to the high amount of peak overlapping

of different phases in this sample. For the other Cr-spinel (GK1C-1), thermal displacement parameters were refined together with the rest of general parameters.

Single crystal studies

Crystal fragments of natural Cr-spinels suitable for single crystal X-ray analyses were used. X-ray diffraction measurements were collected at room temperature by ω-scan technique on an Agilent Oxford Diffraction Super Nova Dual four-circle diffractometer equipped with Atlas CCD detector. X-ray data collection was carried out at room temperature using mirror- monochromatized MoKα radiation micro-focus source (λ=0.7107Å). The determination of unit cell parameters, data integration, scaling and absorption correction were carried out using the CrysAlisPro program package [23]. The structures were solved by direct methods (SHELXS-97) [24] and refined by full-matrix least-square procedures on F^2 (SHELXL-97) [24]. The atomic displacement parameters were refined anisotropically.

Overall six crystal fragments from both Cr-spinel samples were chosen for better statistics. Structure refinements were performed using F_o^2 in space group $Fd\bar{3}m$ (№227) constrained on full site occupancy.

Refined parameters were overall scale factor, extinction coefficient, atomic coordinates, tetrahedral and octahedral site occupancies and atomic displacement parameters U. Refined site occupancies are expressed as mean atomic number (product of atomic fraction and atomic number of chemical species entering both structural positions) in tetrahedral (Td m.a.n.) and octahedral (Oh m.a.n.) sites, respectively.

Obtained cation distribution was additionally refined according to a procedure described by Lavina et al. [21], in which both structural and chemical data (bond lengths, *a*, *u* and atomic proportions) are taken into account. In this procedure the cation distribution is obtained by minimising the differences between observed crystal-chemical parameters (*a*, *u*, Td-O, Oh-O and chemical composition, obtained from structure refinement and EPMA) and those calculated from variable site atomic fractions. The bond lengths were calculated as the linear contribution of each cation multiplied by its ideal bond length at the respective site. The ideal bond lengths for all chemical species known in spinels are well determined on the basis of analysis of more than 290 spinel structural data [21, 22]. During the minimization, the minor cations (Ni^{2+}, V^{3+}, Ti^{4+} and Mn^{2+}) were assigned according to their site preferences and fixed with atomic proportions corresponding to the EPMA data.

Finally, based on cation distributions obtained, we used the geothermometer proposed by Princivalle et al. [25] to calculate system closure temperatures.

RESULTS

SEM and EPMA studies

The Cr-spinel grains in the semi-massive sample (Fig. 2) show clear irregular zoning, with smooth

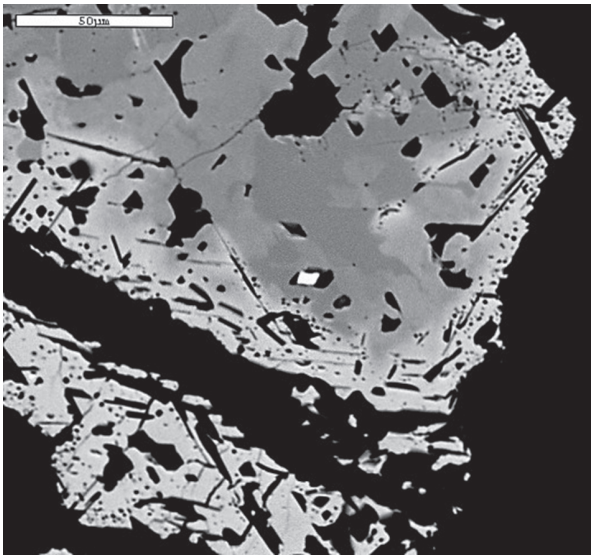

Fig. 2. BSE image of zonal Cr-spinel from the semi-massive sample. Porous rim is richer in Fe^{2+} and Cr.

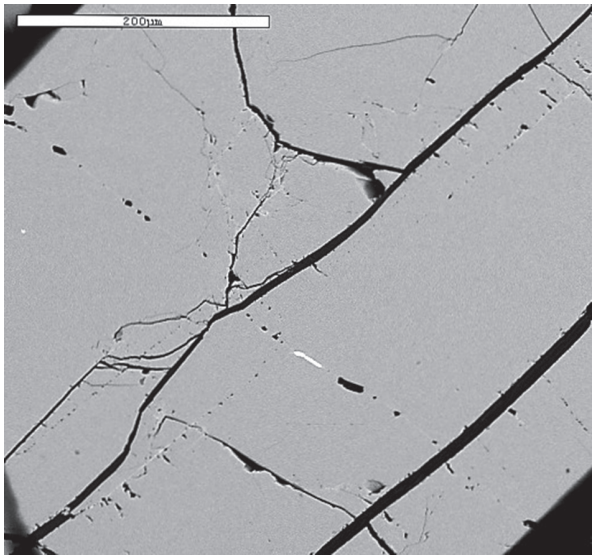

Fig. 3. BSE image of homogeneous Cr-spinel from the massive sample.

cores and pretty porous rims. This zoning is a product of reaction of Cr-spinel with surrounding silicates during retrograde metamorphic alteration [26]. For this reason hereafter we will call this Cr-spinel *zonal*. The mentioned chlorite is the respective silicate side product of the same reaction. Briefly, this alteration is characterized by Mg and Al depletion of Cr-spinel and introduction of extra Fe^{2+} from the silicates.

The Cr-spinel from the massive sample (Fig. 3) shows almost no zoning. For this reason hereafter we will call it *homogeneous*. The visible homogeneity is thought to result from secondary homogenization (magnetitization) during late metamorphic events. EPMA data show that this Cr-spinel is very rich in iron (1.88 *apfu* total Fe) with Cr, Mg, and minor Al contents, approaching magnetite – magnesioferrite joint in the compositional field of Cr-spinels.

Averaged chemical compositions of different Cr-spinel zones (columns 1–4) and bulk (column 5) for the zonal sample as well as bulk Cr-spinel composition for the homogeneous sample (column 6) are given in Table 1.

As seen in this table, zonal Cr-spinel is characterized with high Cr, Al and Mg contents. In core to rim direction a clear trend for Al and Mg depletion, compensated by Fe^{2+} and Cr enrichment are noted, while Fe^{3+}, Mn and minor elements remain fairly constant. This trend of substitution is clearly visible on Fig. 4, where the compositions of the stud-

Table 1. Microprobe data, represented as oxide wt. % and recalculated to pure element values, according to stoichiometry based on 3 cations per 4 oxygen ions. Integral compositional parameters are calculated in the bottom part of the table too

	zonal					homogeneous
Sample label, area and number of points	GK1A-7 core 13p.	GK1A-7 rim1 13p.	GK1A-7 rim2 8p.	GK1A-7 rim3 7p.	GK1A-7 bulk 41p.	GK1C-1 21p.
Al_2O_3	21.570	17.350	13.890	11.010	16.931	0.434
MgO	14.610	13.340	12.310	11.390	13.208	4.705
FeO	12.651	13.937	14.933	15.923	14.063	23.594
Fe_2O_3	4.991	4.751	4.704	4.057	4.700	41.857
MnO	0.415	0.439	0.491	0.530	0.458	0.633
SiO_2	0.031	0.029	0.030	0.037	0.031	0.035
Cr_2O_3	45.380	49.920	53.460	57.050	50.391	27.805
TiO_2	0.071	0.067	0.070	0.066	0.069	0.260
V_2O_5	0.215	0.187	0.192	0.196	0.199	0.135
NiO	0.150	0.116	0.130	0.110	0.128	0.241
∑	100.084	100.136	100.215	100.369	100.178	99.698
Al	0.776	0.641	0.524	0.422	0.624	0.019
Mg	0.666	0.623	0.587	0.552	0.618	0.258
Fe^{2+}	0.326	0.366	0.400	0.434	0.371	0.724
Fe^{3+}	0.113	0.112	0.113	0.099	0.111	1.156
Mn	0.011	0.012	0.013	0.015	0.012	0.02
Cr	1.101	1.238	1.353	1.469	1.255	0.806
Ti	0.002	0.002	0.002	0.002	0.002	0.007
V	0.004	0.003	0.003	0.003	0.003	0.002
Ni	0.004	0.003	0.003	0.003	0.003	0.007
∑	3.001	3.000	2.998	2.999	2.999	2.999
$Fe^{3+}/Fe_{tot.}$avg.	0.261	0.234	0.220	0.186	0.230	0.614
Cr/Fe_{tot}	2.51	2.59	2.64	2.76	2.60	0.43
Cr#=Cr/(Cr+Al) avg	0.585	0.659	0.721	0.777	0.668	0.977
Mg#=Mg/(Mg+Fe^{2+})	0.673	0.630	0.595	0.56	0.625	0.263
Fe#=Fe^{3+}/(Cr+Al+Fe^{3+})	0.06	0.06	0.06	0.05	0.06	0.58
$Cr^{3+}/(Cr^{3+}+ Fe^{3+})$	0.906	0.917	0.923	0.937	0.920	0.411
∑Fe	0.439	0.478	0.513	0.533	0.482	1.88
Fe^{3+}/Fe^{2+}	0.35	0.31	0.28	0.23	0.30	1.60

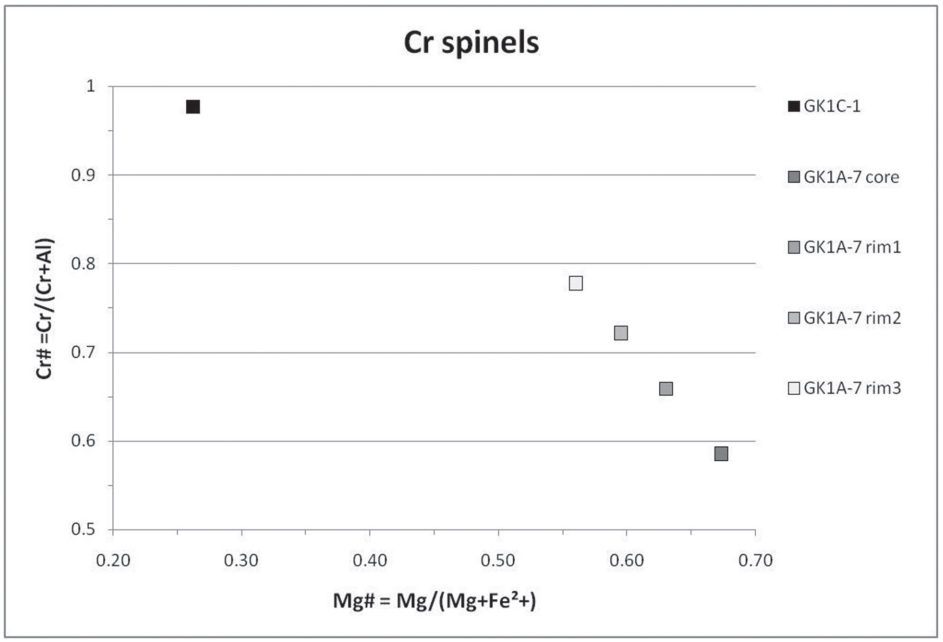

Fig. 4. Mg# vs. Cr# compositional diagram. Sample GK1A-7 (gray squares) is zonal with preserved pristine cores and GK1C-1 (black square) is homogeneous, very rich in iron Cr-spinel.

ied Cr-spinels are presented as Mg# vs. Cr# (Mg# = Mg/(Mg+Fe^{2+}), Cr# = Cr/(Cr+Al), all in at. %). The compositional variations of Al^{3+}, Cr^{3+} and Fe^{3+} are presented on the ternary diagram (Fig. 5), where zonal Cr-spinel forms four clusters (gray squares), corresponding to the 4 zones distinguished on SEM images and also marked by peak splitting in powder X-ray patterns.

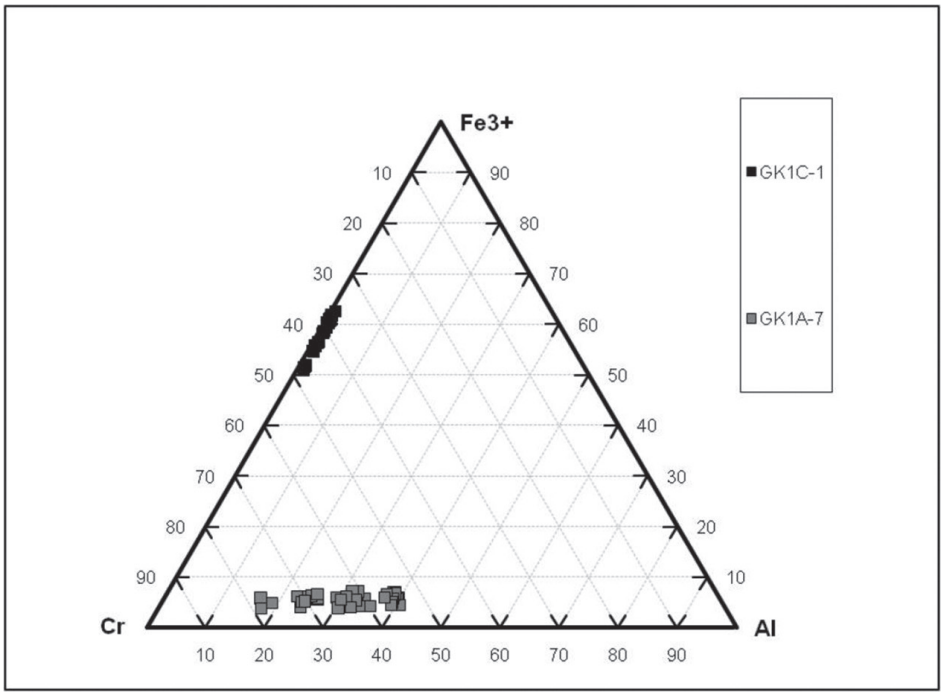

Fig. 5. Compositional variations of Al^{3+}, Cr^{3+} and Fe^{3+} in the studied Cr-spinels.

Mössbauer spectroscopy

The registered Mössbauer spectra include both sextet (Sx) and doublet (Db) components (Table 2). According to literature data the spectra of Cr-spinel samples could be interpreted both considering completely normal cation distribution and intracrystalline cation disorder. Sample GK1C-1 (homogeneous), (Fig. 6) shows three magnetically split sextets together with superposing doublets. The calculated hyperfine parameters clearly show the presence of non-stoichiometric Cr-spinel phases $Fe_{1+x}Cr_{2-x}O_4$ having sextet components typical for compositions with x<0.68. Doublet type components are characteristic for larger x value, as well as for Cr-spinel with small particle size when relaxation effects could also be observed. In the first case the extra iron substitutes Cr in octahedral sites and Fe^{3+} ions in tetrahedral position are registered. In octahedral position the presence of Fe^{3+} and Fe^{2+} ions gives rise to electron hopping [27]. Also the presence of Fe^{3+} and Cr in octahedral sites disturbs the cubic symmetry around the tetrahedrally coordinated Fe^{2+} and hence the Fe^{2+} singlet is converted into a doublet. Quadrupole splitting (QS) increases with increasing Fe^{3+} in octahedral site [28]. Sample GK1A-7 (zonal), (Fig. 7) shows doublet type spectrum, typical for Cr-spinel with high Cr content. The presence of Fe^{3+} in octahedral position and Fe^{2+} in two tetrahedral positions was registered [29].

Table 2. Mössbauer hyperfine parameters, distribution of Fe^{2+} and Fe^{3+} at different sites of Cr-spinels and $Fe^{3+}/\Sigma Fe$ ratios from the spectral areas at 298 K

Sample	Components	IS, mm/s	QS, mm/s	H_{eff}, T	FWHM, mm/s	G, %	$Fe^{3+}/\sum Fe$
GK1C-1	Sx1-Fe^{3+}-tetra	0.29	0.01	48.75	0.35	30	0.645
	Sx2-$Fe^{2.5+}$-octa	0.62	-0.04	46.02	0.47	23	
	Sx3-$Fe^{2.5+}$-octa (CME)	0.70	-0.06	44.11	0.66	26	
	Db1-Fe^{3+}-octa	0.36	0.42	–	0.31	10	
	Db2-Fe^{2+}-tetra	0.94	0.52		0.49	11	
GK1A-7	Db1-Fe^{3+}-octa	0.32	0.56	–	0.50	37	0.37
	Db2-Fe^{2+}-tetra	0.84	1.07	–	0.34	20	
	Db3-Fe^{2+}-tetra	1.10	1.00	–	0.52	43	

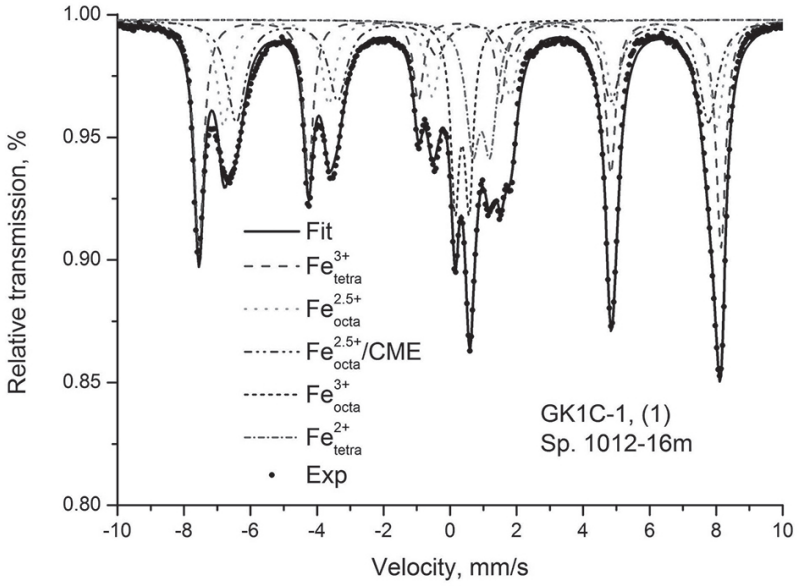

Fig. 6. Mössbauer spectrum of homogeneous Cr-spinel.

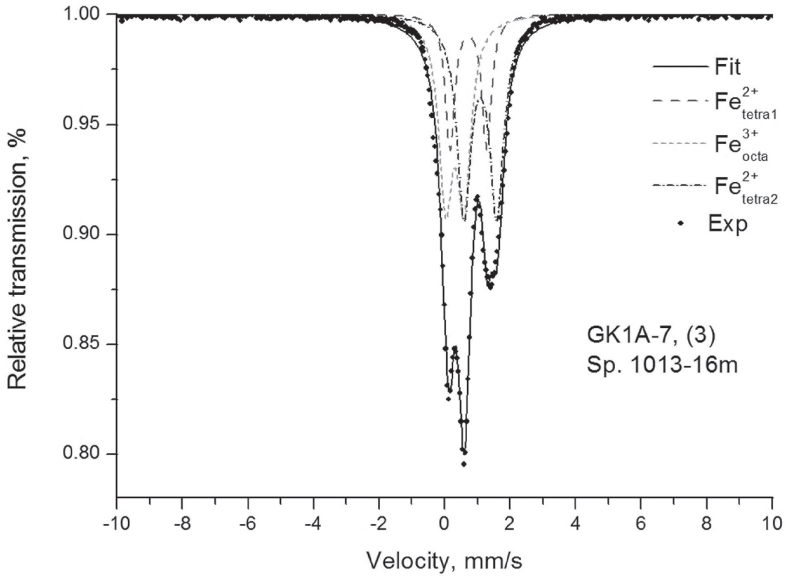

Fig. 7. Mössbauer spectrum of zonal Cr-spinel.

Powder diffraction and Rietveld analysis

Powder X-ray diffraction analysis of the studied Cr-spinels shows that the investigated samples contain only spinel phases. Diffraction patterns for both samples are characterized with some differences, considering intensities, peak positions, FWHM of the peaks and the background level. The homogeneous sample shows narrow peaks and high background, witnessing of good crystallinity and high iron contents. Diffraction pattern of the zonal sample, in contrast, shows spectacular splitting of Bragg reflections, especially observed at high 2θ angles. This splitting reflects the compositional variability already confirmed by EPMA data. Because of strong peak overlapping, however, approximation of profile parameters was very hard. This sample was modeled with 3 phases, despite of indications for four spinel phases. Rietveld refinement was carried out with pseudo-Voigt profile function for zonal sample and TCH (Thompson, Cox and Hastings) pseudo-Voigt function with asymmetry correction by FCJ (Finger, Cox and Jephcoat) for the homogeneous sample. Rietveld plots are shown in Figures 8 and 9. The results from the Rietveld refinement are presented in Table 3.

Single crystal structure refinement

The structure refinement was performed, assuming fully ionized cations and neutral scattering for the oxygen. The distribution of main chemical species and constrained minor elements (Mn, Ni, Ti and V) in tetrahedral or octahedral sites was initially set, according to their site preferences [21]. The results of the refinement are represented in Table 4.

Final cation distributions, based on the procedure of Lavina et al. [21] are given in Table 5.

Intracrystalline geothermometry

In the present study we applied geothermometry calculations decribed by Princivalle et al. [25], which consider the Al and Mg intersite exchange and the chemical composition. The estimated temperatures for some of the studied Cr-spinels are in the range 796–1073°C (Table 5). For the zonal Cr-spinel (with preserved pristine cores) this temperature range could reflect the stage of reequlibration on cooling.

DISCUSSION

The two X-ray diffraction methods used – powder and single crystal, operate with slightly different material. The powder samples use bulk material, while crystal fragments used for single crystal studies, may belong to separate crystal zones. Since these particular zones differ in composition, they can give slightly different X-ray patterns. This is why the results from the single crystal study are slightly spread around the powder (bulk) results. This is well visible on Fig. 10, where solid squares and circles reflect powder and single crystal results, respectively. As seen, regardless of the slight displacements, two kinds of results coincide within rather narrow limits. This coincidence gives us a

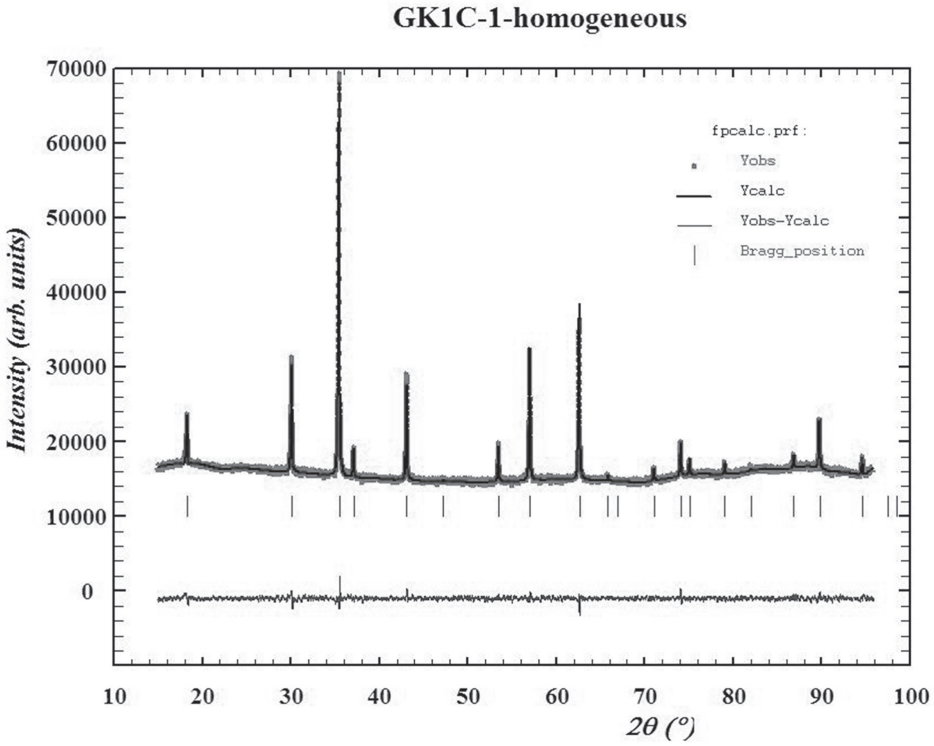

Fig. 8. Rietveld plot of homogeneous Cr-spinel. Vertical bars denote Bragg positions; the dotted curve – experimental diffraction pattern; solid line is the calculated curve and the differences plot is presented at the bottom.

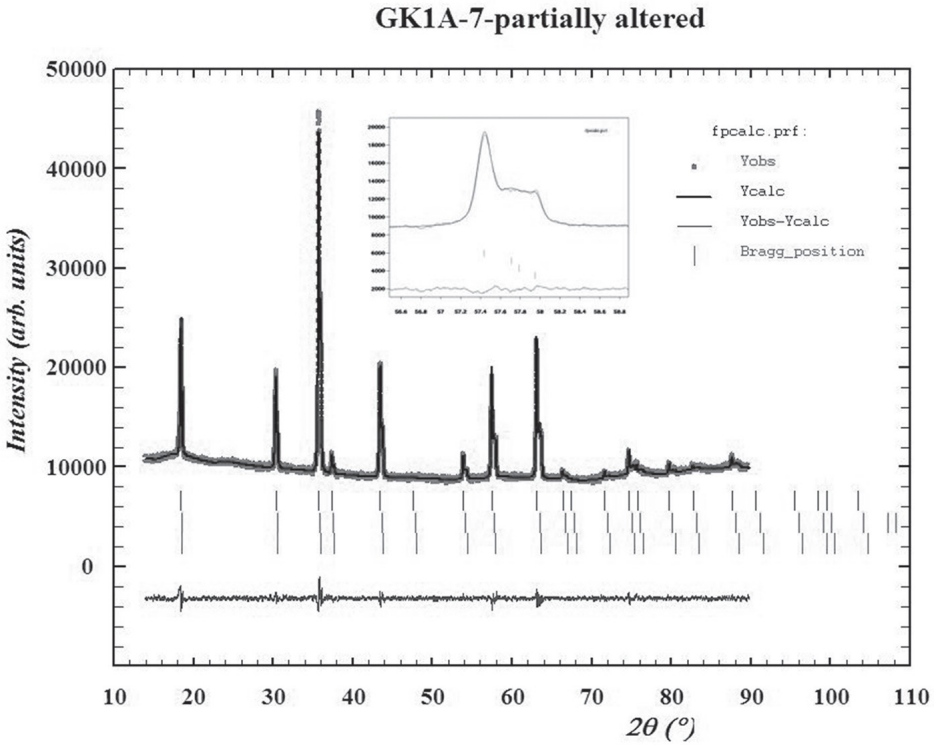

Fig. 9. Rietveld plot of zonal Cr-spinel. Inset shows splitting of the peaks. Line legend as in Fig. 8.

Table 3. Refined structural parameters from Rietveld refinement of the Cr-spinels studied. *a*: unit cell parameter (Å); *u*: oxygen positional parameter; Td-O and Oh-O: tetrahedral and octahedral bond lengths (Å); $Td_{m.a.n.}$ and $Oh_{m.a.n.}$: mean atomic number for tetrahedral and octahedral sites; B_O, B_{Td} and B_{Oh}: isotropic thermal displacement parameters; x: inversion parameter; the standard deviation is denoted in the brackets

Rietveld refinement for powder samples				
Sample	GK1A-7 core	GK1A-7 rim1	GK1A-7 rim2	GK1C-1
a (Å)	8.25974 (5)	8.29103 (7)	8.32591 (5)	8.38598 (1)
u	0.26261 (9)	0.26205 (16)	0.26258 (9)	0.25809 (14)
Vol	563.506 (0)	569.933 (0)	577.159 (5)	589.742 (2)
Dcal *g/cm*³	4.398	4.447	4.482	4.873
Td-O (Å)	1.9687 (12)	1.9689 (6)	1.9840 (4)	1.9331 (6)
Oh-O (Å)	1.9663 (10)	1.9776 (5)	1.9823 (3)	2.0309 (7)
RB	3.69	2.55	2.76	4.35
RF	3.85	2.22	2.72	5.51
Chi2	2.26	2.26	2.26	2.42
GoF	1.5	1.5	1.5	1.6
Rp	22.3	22.3	22.3	22.3
Rwp	10.7	10.7	10.7	13.2
Rexp	7.1	7.1	7.1	8.51
Td m.a.n.	16.89	17.64	17.86	23.65
Oh m.a.n.	20.29	20.91	21.63	24.08
B_O	1.15 (2)	0.92 (9)	0.21 (5)	1.18 (5)
B_{Td}	0.67 (2)	0.69 (6)	0.08 (4)	0.86 (3)
B_{Oh}	0.39 (1)	0.57 (4)	0.64 (3)	0.51 (2)
		Site occupancy		
		Td site		
Mg	0.611 (2)	0.583 (2)	0.547 (1)	0.239 (1)
Fe^{2+}	0.357 (2)	0.397 (2)	0.420 (1)	0.260 (1)
Mn	0.011	0.013	0.015	0.020
Fe^{3+}	0.000	0.000	0.000	0.520 (1)
Al	0.000	0.000	0.000	0.000
total	0.979	0.992	0.982	1.039
vacancy	0.021	0.008	0.018	
∑	1.000	1.000	1.000	
		Oh site		
Al	0.649 (2)	0.573 (2)	0.419 (1)	0.019
Fe^{3+}	0.113 (2)	0.112 (2)	0.099 (1)	0.636 (1)
Fe^{2+}	0.023 (2)	0.000	0.000	0.465 (1)
Mg	0.000	0.000	0.000	0.000
Cr	1.182 (2)	1.302 (2)	1.460 (1)	0.786 (1)
Ni	0.004	0.003	0.003	0.007
Ti	0.002	0.002	0.002	0.007
V	0.004	0.003	0.003	0.003
total	1.977	1.994	1.986	1.923
vacancy	0.023	0.006	0.014	0.077
∑	2.000	2.000	2.000	2.000
x	0.000	0.000	0.000	0.52

reason to trust both study results. Moreover, both results comply well with EPMA and Mössbauer results.

The same figure shows clear clustering of data points from the homogeneous (black symbols) and zonal (gray symbols) Cr-spinels.

The homogeneous Cr-spinel points cluster close to magnesioferrite position (MgFt), giving us reason to classify this sample as such. Its *u* value below 0.26 witnesses for partially inverse character. This fact well corresponds to its high Fe content (both Fe^{2+} and Fe^{3+} derived from Mössbauer results).

Table 4. Single crystal structure refinement results. *a*: unit cell parameter (Å); *u*: oxygen positional parameter; Td-O and Oh-O: tetrahedral and octahedral bond lengths (Å); $Td_{m.a.n.}$ and $Oh_{m.a.n}$: mean atomic number for tetrahedral and octahedral sites; U_{11} and U_{12}: anisotropic thermal displacement parameters for Td, Oh and O (oxygen) sites

SHELXL refinement - Sheldricks 2013						
Sample	GK1A-7m -1a	GK1A-7m -1b	GK1A-7m -1c	GK1C-1-3a	GK1C-1-3b	GK1C-1-3c
a (Å)	8.2483 (4)	8.2936 (3)	8.2827 (4)	8.3784 (4)	8.3854 (5)	8.4021 (5)
u	0.26256 (14)	0.26201 (14)	0.26170 (18)	0.2577 (3)	0.2591 (5)	0.2588 (6)
cell vol	561.17 (8)	570.47 (6)	568.22 (8)	588.14 (8)	589.62 (11)	593.15 (11)
Td-O	1.965 (2)	1.968 (2)	1.961 (3)	1.926 (5)	1.948 (8)	1.9473 (8)
Oh-O	1.9639 (10)	1.9788 (10)	1.9785 (13)	2.032 (3)	2.023 (4)	2.0292 (4)
O-Oh-O shared	83.80 (7)	84.09 (7)	84.25 (9)	86.31 (17)	85.6 (3)	86.2 (2)
O-Oh-O unshared	96.20 (7)	95.91 (7)	95.75 (9)	93.69 (17)	94.4 (3)	93.8 (2)
Td m.a.n	15.89	16.86	16.98	23.48	22.38	25.50
Oh m.a.n.	18.57	19.75	19.82	24.12	24.98	25.16
U_{11}(Td)	0.0050 (6)	0.0065 (5)	0.0075 (7)	0.0048 (12)	0.0060 (13)	0.0064 (13)
U_{11}(Oh)	0.0034 (4)	0.0030 (3)	0.0044 (4)	0.0041 (9)	0.0118 (13)	0.0127 (13)
U_{12}(Oh)	0.00014 (16)	-0.00025 (14)	-0.0003 (2)	-0.0003 (5)	-0.0003 (5)	-0.0004 (7)
U_{11}(O)	0.0076 (7)	0.0087 (7)	0.0091 (9)	0.007 (2)	0.012 (3)	0.009 (3)
U_{12}(O)	0.0006 (4)	0.0003 (4)	-0.0001 (6)	0.0006 (17)	0.0006 (17)	0.0021 (19)
N refl	49	50	51	53	54	55
R all	0.0152	0.0137	0.0203	0.0193	0.0497	0.0619
R1	0.0146	0.0128	0.0195	0.0157	0.0477	0.0525
wR2	0.0334	0.0291	0.0371	0.0951	0.1424	0.1555
GoF	1.171	1.11	1.256	0.953	1.304	1.318
ext *coeff*	0.0074 (11)	0.0006 (5)	0.0000 (6)	0.0005 (14)		
abs *coeff* μ	3.576	3.518	3.532	3.354	3.346	3.326
Z	8	8	8	8	8	8

Points from the zonal Cr-spinel show much wider spread of *a* unit cell values, at almost constant *u*. This means that compositional differences (registered also by EPMA) between crystal core and rims result in different unit cells, but do not significantly affect the oxygen positional parameter. This behavior is not surprising. It was registered before by Lenaz and Princivalle [6] and allows pretty precise determination of *u*, regardless of possible spread in *a* values within certain limits.

Clear clustering of the two samples well apart is also visible on the tetrahedral (Td-O) vs. octahedral (Oh-O) bond length diagram (Fig. 11). The homogeneous Cr-spinel points (black symbols) cluster again close to the magnesioferrite position, but show somewhat larger tetrahedral and shorter octahedral bonds. This perfectly makes sense since extra Fe^{2+} (introduced during alteration) in tetrahedral position has much larger ionic radius than Mg. Chromium in octahedral position is smaller than Fe^{3+}, but the difference here is smaller, which well explains smaller deviation from magnesioferrite values.

The zonal sample (gray symbols) shows abrupt increase in octahedral bond length in core to rim direction, followed by bilateral spread in tetrahedral distances between different rims. The first change reflects the growing Cr/Al ratio, in octahedral position. Intra-rim differences are entirely due to variations in Fe^{2+}/Mg ratio, in tetrahedral position.

Finally, calculated cation distribution values were used for calculation of system closure temperatures, in accordance with the geothermometric procedure of Princivalle et al. [25]. Obtained temperatures for the zonal Cr-spinel were in the range 796–1073°C. Slightly lower temperatures were calculated for the homogeneous Cr-spinel 940–955°C. These temperatures are completely acceptable for a reequilibration stage (pristine cores) and very close to the temperatures reported for chromites from the Outer Dinarides [6]. Outer alteration rims of zonal sample are expected to have formed at much lower temperatures, during regional metamorphism (700–450°C) [26], but they were not calculated in this study, since used geothermomertic procedure is based on melt crystallization concepts, inapplicable for hydrothermal environment of the metamorphic stage.

Table 5. Final cation distributions refined according to the procedure of Lavina et al. [21]

Sample	GK1C-1 powder	GK1C-1-3c	GK1A-7m-1a	GK1A-7m-1b	GK1A-7m-1c
		Calculated cation distribution			
a (Å)	8.385869	8.402383	8.2483	8.2936	8.2827
u	0.258089	0.258796	0.26254	0.26200	0.2617
Td-O	1.93309	1.947189	1.965	1.9680	1.9611
Oh-O	2.030906	2.029386	1.9641	1.9789	1.9785
Td m.a.n.	22.75	22.75	15.82	16.69	16.09
Oh m.a.n.	24.62	24.98	18.87	20.09	20.30
Total charges	7.97	7.97	7.95	7.85	7.90
		Site occupancy			
		Td site			
Mg	0.229	0.232	0.677	0.617	0.643
Fe^{2+}	0.235	0.350	0.247	0.320	0.258
Mn	0.020	0.005	0.011	0.012	0.01
Fe^{3+}	0.515	0.413	0.012	0.000	0.022
Al	0.000	0.000	0.053	0.051	0.065
Sum	0.999	1.000	1.000	1.000	0.998
Vacancy	0.001	0.000	0.000	0.000	0.002
		Oh site			
Al	0.019	0.022	0.903	0.687	0.698
Cr	0.809	0.866	0.873	1.109	1.115
Fe^{3+}	0.647	0.650	0.109	0.003	0.000
Fe^{2+}	0.461	0.455	0.054	0.151	0.175
Mg	0.029	0.000	0.055	0.040	0.006
Ni	0.007	0.002	0.002	0.002	0.002
Ti	0.007	0.005	0.001	0.002	0.001
V	0.002	0.000	0.003	0.002	0.002
Sum	1.980	2.000	2.000	1.996	1.999
vacancy	0.020	0.000	0.001	0.004	0.001
x	0.515	0.413	0.065	0.051	0.087
T°C	940	955.15	796.00	982.86	1073.41
$Fe^{3+}/\Sigma Fe$	0.625	0.569	0.287	0.006	0.048

CONCLUSIONS

Based on structural, chemical and Mössbauer data collected, the two samples used in this study were identified as:

- Magmatic Cr-spinels, with high Al cores and progressively depleted in Al and less Mg alteration rims.
- High chromian magnesioferrite, which is a partially inverse Cr-spinel, not described previously in this locality. This determination was only possible with structural refinement, combined with Mössbauer data and demonstrated the importance of such studies for the correct mineral species identification in metamorphosed ophiolite sequences.

The two X-ray diffraction approaches – powder and single crystal gave comparable results, which makes them interchangeable for the purposes of this kind of studies. However some aspects of the structural characterization are better revealed by one or the other method and using them both gives best results.

REFERENCES

1. R. J. Hill, J. R. Craig, G. V. Gibbs, *Phys. Chem. Minerals,* **4**, 317 (1979).
2. F. Bosi, G. B. Andreozzi, V. Ferinni, S. Lucchesi, *Amer. Miner.*, **89**, 1367 (2004).
3. G. B. Andreozzi, *Per. Mineral*., **68** (1), 43 (1999).
4. D. Lenaz, H. Skogby, F. Princivalle, U. Hålenius, *Phys. Chem. Minerals.*, **31**, 633 (2004).
5. R. O. Sack, M. S. Ghiorso, *American Mineralogist*, **76**, 827 (1991).

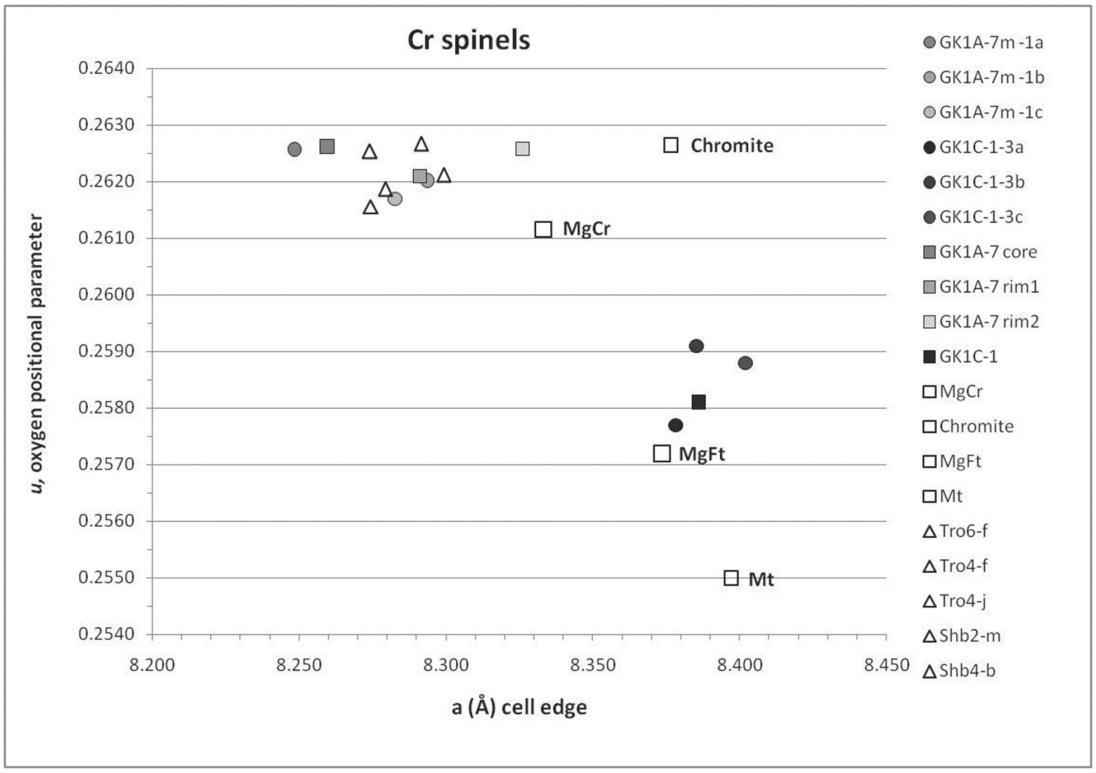

Fig. 10. Oxygen positional parameter vs. unit cell edge. Synthetic and natural Cr-spinels fom literature sources are presented for comparison too. Solid circles = single crystal data; solid squares = Rietveld refinement data; empty squares = chromite, magnesiochromite, magnesioferrite [30], and magnetite [31]; empty triangles = Albanian chromite [2]); MgCr = magnesiochromite; Mt = magnetite; MgFt = magnesioferrite.

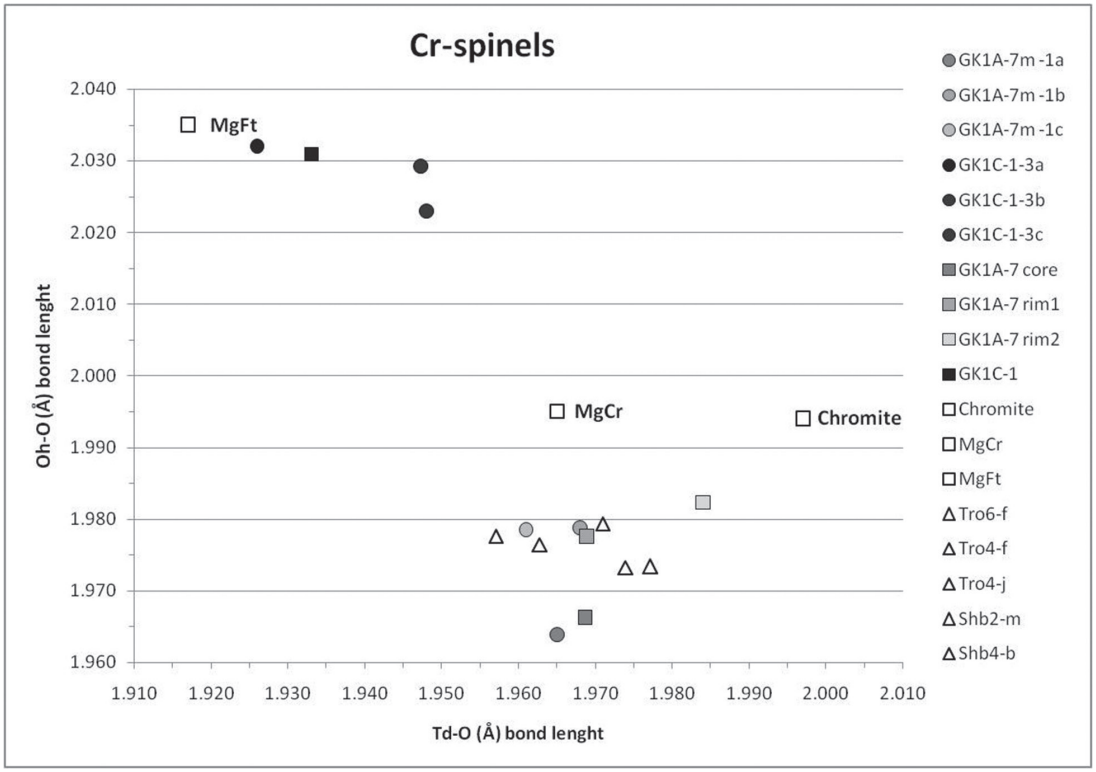

Fig. 11. Tetrahedral (Td-O) and octahedral (Oh-O) bond lengths. The symbols and notations are same as in Fig. 10.

6. D. Lenaz, F. Princivalle, *The Canadian Mineralogist*, **43**, 1305 (2005).
7. B. Lavina, B. Cesare, A. M. Álvarez-Valero, Hinako Uchida, R. T. Downs, A. Koneva, P. Dera, *American Mineralogist*, **94**, 657 (2009).
8. K. Kolcheva, I. Haydoutov, L. Daieva, *Geochem Mineral Petrol*, **37**, 25 (2000).
9. I. Haydoutov, K. Kolcheva, L. A. Dieva, I. Savov, C. Carrigan, *Ofioliti*, **29** (2), 145 (2004).
10. N. Bonev, in: Geol Soc Am Special Paper, Dilek Y, Pavlides S (eds). **49**, 211 (2006).
11. E. Mposkos, A Liati, *Can Mineral*, **31**, 401 (1993).
12. L. Macheva, *Geochem Mineral Petrol*, **35**, 17 (1998).
13. E. Mposkos *Bull Geol Soc Greece*, **32**, 59 (1998).
14. E. Mposkos, *Bull Geol Soc Greece*, 34, 2126 (2002).
15. E. Kozhoukharova, *Geochem Mineral Petrol*, **35**, 29 (1998).
16. S. Sarov, B. Yordanov, V. Valkov, S. Georgiev, D. Kamburov, E. Raeva, V. Grozdev, E. Balkanska, L. Moskovska, G. Dobrev, E. Voynova, M. Ovcharova (2007) Geological map of the republic of Bulgaria 1:50000: scheet K-35-88-V (Krumovgrad) and K-35-100-A (Egrek). Ministry of Environment and Water, Bulgarian geological Survey, project Nr. 425/20.07.2004, Geology and Geophysics JSCo., Apis 50 Ltd. printhouse. Sofia.
17. C-J De Hoog, *Geochem Geophys Geosyst*, **10**: Q10014 (2009).
18. T. Žák, Y. Jirásková, *Surf. Interface Anal.* **38**, 710 (2006).
19. MATCH!, Crystal Impact, H.Putz & K.Brandenburg GbR, Bonn, Germany, 2003-2016.
20. J. Rodriguez-Carvajal, *Physica* B., **55**, 192 (1993).
21. B. Lavina, G. Salviulo, A. Della Giusta, *Phys Chem. Minerals.*, **29**, 10 (2002).
22. H. O`Neill, A. Navrotsky, *American Mineralogist*, **68**, 181 (1983).
23. Oxford Diffraction. CrysAlis PRO, Oxford Diffraction Ltd, yarnton, England, 2010.
24. G. M. Sheldrick, *Acta Crystallographica A*, **64**, 112 (2008).
25. F. Princivalle, A. Della Giusta, A. De Min, E. M. Piccirillo, *Mineral. Mag.*, **63** (2), 257 (1999).
26. F. Gervilla, J. A. Padron-Navarta, T. Kerestedjian, I. Sergeeva, J. M. Gonzalez Jimenez, I. Fanlo, *Contrib. Mineral. Petrol.,* **164**, 643 (2012).
27. D. Lenaz, G.B. Andreozzi, M. Bidyananda, F. Princivalle, *Periodico di Mineralogia,* **83** (2), 241, 10.2451/2014PM0014, (2014).
28. H. C. Verma, J. K. Mohanty, R. P. Tripathi, *Journal of Alloys and Compounds*, **326**, 132 (2001).
29. Y. L. Chen , B. F. Xu , J. G. Chen and Y. Y. Ge, *Phys Chem Minerals*, (**19)**, 255 (1992).
30. D. Lenaz, H. Skogby, *Per. Mineral.*, **72**, 69 (2003).
31. H. St. C. O'Neill and W. A. Dollase, *Phys Chem Minerals*, (**20**), 541 (1994).

КРИСТАЛОХИМИЯ И СТРУКТУРНО ХАРАКТЕРИЗИРАНЕ НА ПРИРОДНИ ХРОМШПИНЕЛИДИ

И. С. Сергеева[1*], Т. Н. Керестеджиян[1], Р. П. Николова[2], З. П. Черкезова-Желева[3], Ф. Хервия[4]

[1] Геологически институт „Страшимир Димитров", Българска академия на науките, бл. 24, 1113 София
[2] Институт по минералогия и кристалография, Българска академия на науките, бл. 107, 1113 София
[3] Институт по катализ, Българска академия на науките, „Акад. Г. Бончев" бл. 11, 1113 София, България
[4] Университет на Гранада, Катедра по минералогия и петрология, 18002 Гранада, Испания

Постъпила октомври, 2016 г.; приета декември, 2016 г.

(Резюме)

Изследвани са два образеца от природни хром шпинелиди посредством рентгеноспектрален микроанализ, прахова и монокристална рентгенова дифракция и Мьосбауерова спектроскопия, с цел установяване на някои аспекти от взаимовръзката между химичният състав и кристалоструктурните параметри. Образците се различават значително в текстурно, химично и структурно отношение. Единият е богат на хром и може да се отнесе като хром шпинелид, докато другият е с високи съдържания на желязо доближавайки се до магнезиоферитовия член от шпинелова група. Различният химизъм поражда отчетливи разлики и в структурните параметри – параметър на елементарната клетка и кислороден параметър, които отразяват различни условия на образуване и/или промяна. Кислородният параметър е индикативен за термичната история на вместващите скали (температура на затваряне на системата) и е пряко свързан с катионното разпределение в структурата – основа за геотермометрични изчисления. Получените температури на затваряне на системата за двата образеца показват стойности в интервала 796–1073 °C, които са приемливи за преуравновесяване на хром шпинелида по време на охлаждане.